This is the Pre-Published Version.

P. Sun, X. Huang, C. Xu (2022) *Flashpoint and Burning of Thin Molten Plastic Pool Above Hot Boundary*, **Applied Thermal Engineering**, 215, 118931. https://doi.org/10.1016/j.applthermaleng.2022.118931

Flashpoint and Burning of Thin Molten Plastic Pool Above Hot Boundary

Peiyi Sun[a,b], Xinyan Huang[a,*], Cangsu Xu[c]

[a] *Research Centre for Fire Safety Engineering, Department of Building Environment and Energy Engineering, The Hong Kong Polytechnic University, Kowloon, Hong Kong*

[b] *The Hong Kong Polytechnic University Shenzhen Research Institute, Shenzhen, China*

[c] *College of Energy Engineering, Zhejiang University, Hangzhou, China*

*Corresponding to xy.huang@polyu.edu.hk (X. Huang)

Abstract: The melting and dripping of burning thermoplastics can cause a new ignition and form a plastic pool fire, resulting in a significant fire risk. This work investigates the burning dynamics of polyethylene (PE) vs polypropylene (PP) pools fully melted at 380-410 ℃ on a hot plate with a controlled area and initial temperature. For PE, three burning patterns are observed and defined under different bottom boundary temperatures. When the boundary temperature is lower than the melting point of thermoplastic, burning Pattern I (near-limit flame) appears shortly and extinguishes quickly. Above the melting point of PE, the flame becomes stronger and can last for the longest period before quenching (Pattern II: transitional flame). PP does not have this transitional-flame stage due to a higher melting point and lower pyrolysis point. When the plastic pool temperature exceeds its flashpoint of about 300 ℃ (~60 ℃ below its pyrolysis point), the flame becomes intense and quickly burns out the molten pool (Pattern III: intensive flame). The burning processes of molten thermoplastics show a clear difference from the burning of ethanol and paraffin wax. This study promotes the understanding of the melting and burning of plastics in real fire scenarios and helps quantify the hazards of dripping and flooring fires.

Keywords: *molten thermoplastics; hot plate; burning dynamics; flame extinction; pool fire*

Highlights

- The ignition and burning dynamics of thin thermoplastic pool fire are explored above a hot boundary.
- Flashpoints of both PE and PP plastic pools are measured to be about 60 ℃ below its pyrolysis point.
- Three burning patterns, (I) near-limit flame, (II) transitional flame, and (III) intensive flame, are found.
- Different burning features between conventional liquid fuels and plastic fuels are compared.

Nomenclature

Symbols		**Greeks**	
A	area (mm^2)	δ	thickness (mm)
B	mass transfer number (-)	γ	pixel ratio
Bi	Biot number (-)	ν	stoichiometric air-fuel ratio (-)
c_p	specific heat (kJ/kg/K)	ρ	density (kg/m^3)
h	convection coefficient (W/m^2-K)		
Δh_c	heat of combustion (MJ/kg)	**Subscripts**	
Δh_{py}	heat of pyrolysis (MJ/kg)	*cond*	conduction
k	thermal conductivity (W/m-K)	*c*	cooling
$\dot{m}''$	mass flux (g/m^2-s)	*ex*	external
Nu	Nusselt number (-)	*f*	flame
$\dot{q}''$	heat flux (kW/m^2)	*F*	fuel
Q	thermal inertia	*i*	inner
Ra	Rayleigh number (-)	*p*	polymer
t	time (s)	*py*	pyrolysis
T	temperature (°C)	*r*	remaining
T_b	boundary temperature (°C)	*u*	up

1. Introduction

The thermoplastic material has an increasing market share in every part of our daily lives (e.g. building, manufacturing, cloth, vehicle and necessities) in view of its low cost and good ductility. Thermoplastics, such as polyethylene (PE), polyethylene chloride (PVC), polypropylene (PP) and expanded polystyrene (EPS), can repeatedly deform and reshape at high temperatures. Thus, they can undergo softening, melting, flowing and pyrolysis processes, so they are different from thermosets [1]. Nevertheless, as a by-product of petroleum, plastics are flammable in nature, and the burning of plastics contributes significantly to the fire intensity and toxic smoke. Driven by the gravity and surface tension forces, the hot molten plastics in fire tend to generate discrete drips or merge into a dripping stream, showing complex fire behaviours. Then, the flame can move with molten plastics, burning as extensive pools, as observed in the 2017 London Grenfell Tower fire [2]. The dripping and pooling of thermoplastics accelerate the flame spread and pose significant fire safety challenges [3,4] (Fig. 1).

The thermoplastics have specific fire behaviours mainly due to the melting and dripping processes [5,6]. Previous studies show that the melting process of thermoplastics has a great impact on ignition [7] and fire spread [8], and the melting of burning plastics could generate the plastic drips with flame, named dripping fire [9–11]. Regarding the fire hazard of melting and dripping plastics, the standard fire tests, e.g. UL-94 [12] and EN-13823 [13], have highlighted the dripping ignition phenomenon in

material classification. Many researchers have measured the mass, size and temperature of drops from burning a vertically oriented plastic sample, based on the UL-94 polymer vertical burning test [14–17]. Numerical modelling has successfully predicted the drip size, generating time [18], and the subsequent free fall process with flame shedding [19]. The continual dripping flame is capable of starting a new fire after landing on other fuels [20]. As revealed in our recent works, dripping ignition is a type of pilot ignition where the ignition of thin fuel follows the classic thermally thin ignition theory [9]. In addition, the property of target materials, such as permeability, also plays an essential role in affecting the dripping ignition process [10].

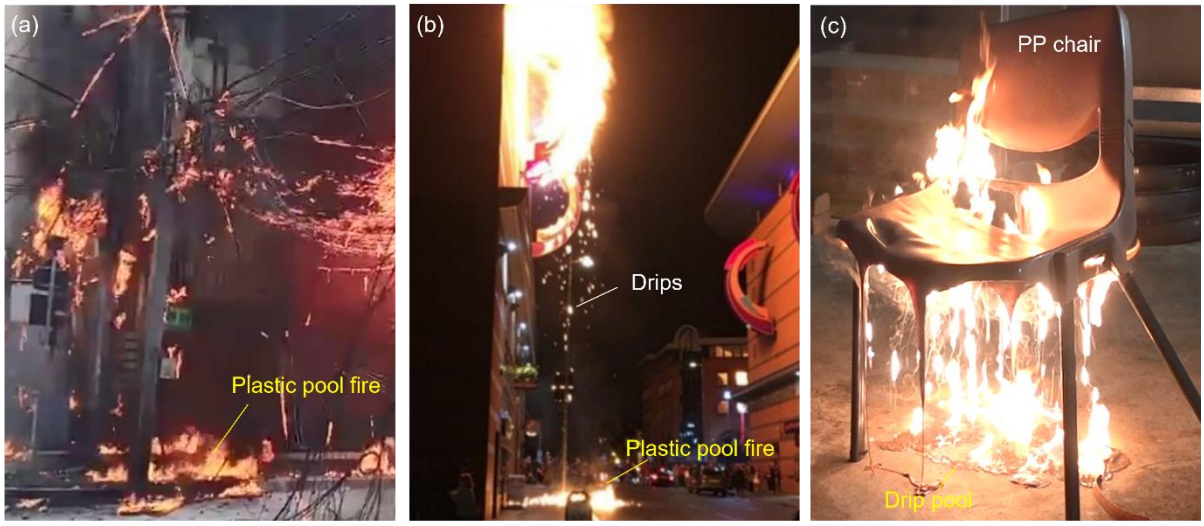

Fig. 1. (a) Plastic pool fire in a real cable fire accident [21] (b) The plastic advertising light caught fire and formed a drip pool at ground [22], and (c) pooling of burning PP chair.

Most past studies focused on the discrete dripping behaviour. However, when the burning of thermoplastics becomes intensive, a large number of drips is generated. Then, they tend to merge into dripping streams and form a pool fire on the ground, expanding the fire hazard [15]. Statistics show that over 74% mass loss of plastics in fire accidents were consumed by plastic pool fires [23,24]. Considering thermoplastics are solid at room temperature and have high melting and pyrolysis points, so their pool fire will be different from either solid fuel (e.g., wood and wax) or liquid fuel (e.g., ethanol or oils). Consequently, it is necessary to investigate the burning behaviour of thermoplastic pool fire. Xie *et al.* [25] designed a novel T-shape trough to investigate flooring and dripping flow behaviour. By measuring the flowing speed of several thermoplastics, PE showed a higher fire risk because of a faster expansion of plastic pool fire [26].

Several large-scale tests investigated the loop mechanism between the plastic wall fire and the plastic pool fire [26,27] and the radiant heat flux [28]. So far, limited studies have discussed the burning of melted plastics in the early fire stage and the influence of ground temperature. The boundary temperature is one of the crucial parameters in the study of conventional pool fires [29]. Moreover, in practical dripping fire scenarios, the ground temperature would increase from the room temperature to

over 600 ℃ in compartment fire [30]. Therefore, this study aims to investigate the boundary temperature effects on burning thermoplastic metals and explore the differences between burning molten plastics and simple solid/liquid fuels.

In this work, the thermoplastics are preheated uniformly in a sealed furnace to generate melts before dripping and ignition on the ground. Then, we focus on the flashpoint of molten plastic and the effect of ground temperature on the burning dynamics and patterns of a plastic pool fire. For comparison, the burning of another two simple fuels, wax and ethanol with different melting points, is also tested to determine the uniqueness of plastic pool fire, and the fire hazard of dripping fire can be determined.

2. Experimental setup

2.1. Plastic drips and pool fire

This work tested two typical thermoplastics, PE and PP, while their melts were burning in a ceramic crucible with a 30-mm diameter and controlled boundary temperature, as shown in Fig. 2. Before experiments, plastic melts were generated by adding a fixed volume of plastic pellets into a customized furnace. The sealed furnace was a cylindrical shape and had an efficient volume of 15 mL. It was powered by six uniformly distributed rod heaters, so that the plastic pellets could be uniformly heated and melted into a fluid. Each time, 2.6 g PE or 2.0 g PP was filled into the furnace and fully molten.

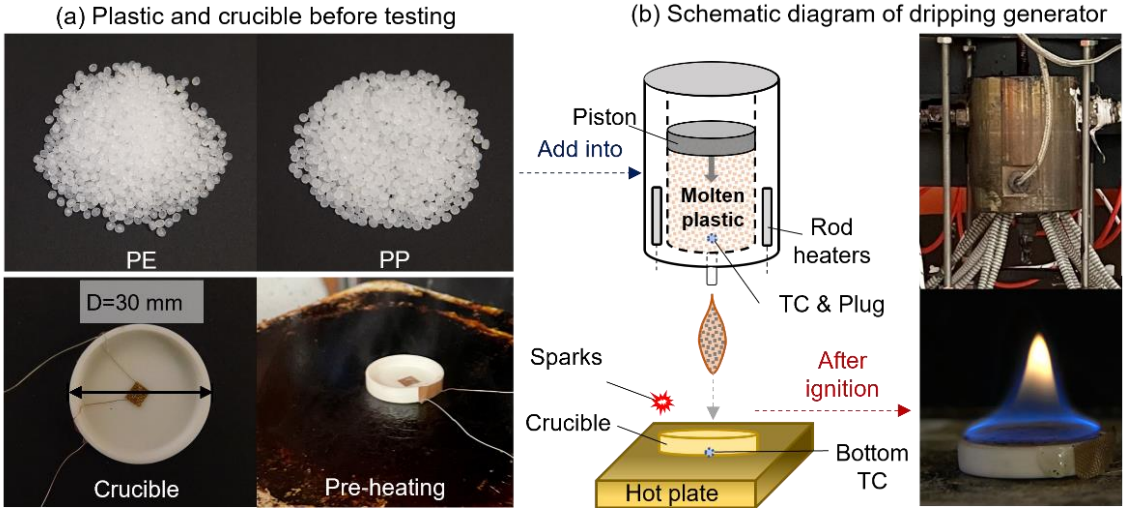

Fig. 2. Experimental setup (a) materials and crucible before testing and (b) the thermoplastic melts and drips generator and the hot plate for controlling boundary temperature.

PE has a higher pyrolysis point (370 ± 10 ℃) than the 340 ± 10 ℃ of PP [31], as found from the thermo-gravimetric analysis (TGA) in Fig. A1 of Appendix. Therefore, the preheating temperature was set to 410 ℃ for PE pellets and 380 ℃ for PP to generate the completely liquified melts, and ensure the melts can be ignited after dripping [25]. The DSC curves in Fig. A1 show that PE also has a melting point (or flowing temperature) of 130 ℃, which is lower than the 180 ℃ of PP [32]. Thus, PE needs a lower temperature to overcome its viscous and surface tension forces to flow freely. The

physicochemical properties of PE and PE are summarized in Table 1.

A thermocouple probe with a 1.5-mm diameter was inserted from the bottom dripping tube, which could monitor the temperature of melts and act as a plug to prevent the leakage of melts. When the melts reached the target temperature, the piston would squeeze all melts out of the vessel through the dripping tube to generate the dripping flow.

After a free fall of 20 cm, the dripping melts were collected by a thin-wall disc crucible of 30 mm diameter. Thus, the initial thickness of molten plastic was fixed to 4.8 mm for PE and 4.5 mm for PP. The diameter of the crucible was 30 mm, which was six times greater than its depth, so that the dominating heat transfer process was in the depth direction and approximately 1D. The calculated Biot Number ($Bi = h_{ex}/h_{in}$) was smaller than 0.1, so the thin plastic pool had a uniform temperature.

This crucible fixed the burning area of the formed plastic pool and was placed above the hop plate. The temperature uncertainty of the hot plate is ± 1 ℃. A thin thermocouple (with a 0.1-mm bead diameter) was fixed on the bottom of the cylinder crucible to measure the temperature of a thin plastic pool. The accuracy of thermocouple is 0.1 ℃. The plastic pool temperature was slightly higher than the set hot-plate temperature, and the pool is too small to affect the hot-plate temperature. Right after landing, the plastic pool was still above the pyrolysis temperature; thus, it had a good flowability and could be piloted easily. This study adopted a spark to pilot a flame on the dripped plastic pool. Note that the spark only acts as the pilot source, which can avoid transporting additional energy to the dripping melts. In this way, the initial condition of dripping melts is well controlled. The spark is applied immediately after dripping and will be removed once the flame ignition is observed.

Table 1. Properties of four fuels at standard conditions (1 atm and 0 ℃) [33–37].

Drip Type	**PE**	**PP**	**Paraffin Wax**	**Ethanol**
Density, ρ (kg/m^3)	920	900	913	757
Specific Heat, c_p (kJ/kg-k)	2.3	2.4	2.6	2.46
Thermal conductivity, k (W/m-K)	0.4	0.11	0.23	0.16
Melting point, T_m (℃)	115	155	48-68	-114
Pyrolysis point, T_{py} (℃)	370 ± 10	340 ± 10	-	-
Boiling point, T_{boil} (℃)	-	-	330-370	78
Flashpoint, T_{flash} (℃)	310 ± 10	260 ± 10	270 ± 10	13
Initial layer thickness, δ (mm)	4.8	4.5	5.0	5.0
Bi (-)	0.02	0.05	0.02	0.03

2.2. Measurements and controlling parameters

In the experiment, the hot plate temperature was varied to investigate the burning behaviours of the plastic pool. The hot plate controlled the bottom surface temperature (T_b) of the crucible that varied from 25 ℃ to 450 ℃, which was measured and calibrated by its default temperature sensor.

Measurements showed that before extinction, the temperature of thin-layer fuel was within 10 ℃ of the set bottom boundary temperature. The plastic residue after extinction was measured by the scale with 0.001 g accuracy. A digital camera was applied to record the burning phenomenon. We can further abstract the flame sustained time and the flame features based on the video. In addition, an infrared camera was used to measure the temperature of plastic pool surface and check its uniformity.

For comparison, two simple hydrocarbon fuels, pure paraffin wax (C_nH_{2n+2}) and ethanol (C_2H_6O), were also burned in the same crucible under the controlled boundary temperature. The ethanol has a very low melting point, so it is liquid at room temperature. The melting point of wax is above 48 ℃, so it is a solid fuel at room temperature. Exactly 2.8 g ethanol or 3.2 g wax was added to the preheated crucible during the test. Then, the initial thickness of the fuel is the same as the depth of the crucible, which is 5 mm. Their detailed properties are summarized and compared in Table 1.

3. Experimental results

3.1. Burning patterns

For thermoplastics, their low melting point and high pyrolysis temperature show unique burning behaviours, different from either non-flow thermosets or pure liquid fuels. In this experiment, the preheating temperatures of thermoplastics are over 200 ℃ higher than their melting point and above their pyrolysis temperature. Thus, the produced molten plastic is highly fluid, and its dripping flow is accompanied by white smoke (i.e., re-condensed pyrolysis gases). After dripping on the hot surface, the drips are still in a high temperature and highly fluid, so they are flooring around the surface to increase the surface area, driven by gravity (see Fig. 3a). At the same time, the landed molten plastic is gradually cooled by the cold bottom boundary surface and eventually re-solidified, where the whole process has no flame due to the lack of a pilot source.

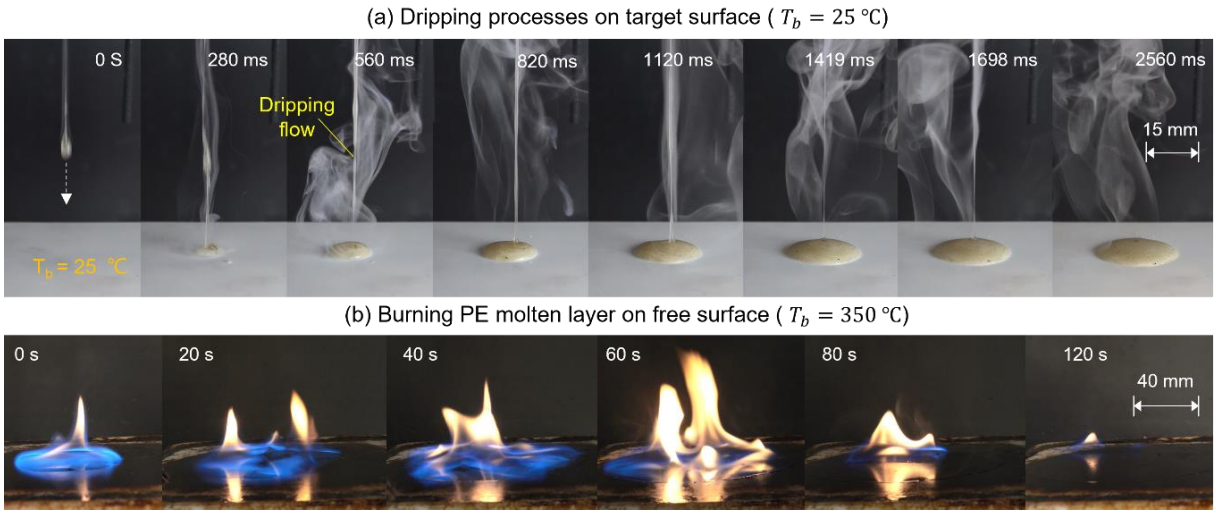

Fig. 3. (a) The dripping, free landing, and flooring processes of molten PE on a cold surface of 25 ℃, and (b) increasing burning area of PE molten layer on the hot plate of 350 ℃ (see Video S1).

A flame will be ignited if a pilot spark is applied immediately after the dripping (see Fig. 3b), because the dripped melts are still higher than the pyrolysis temperature. The molten layer will burn more stably and intensively as the hot-boundary temperature increases. Then, the burning area will also increase dramatically along with the flooring and burning progress, because the surface tension of melts is reduced quickly under the flame heating. In short, the free burn on the hot boundary is extremely complex due to the motion and uniform melts and the changing fuel area and thickness. Therefore, this study collects and burns the dripped plastic melts in a thin-layer crucible to guarantee a uniform fuel surface and constant burning area.

The bottom boundary temperature has a crucial impact on the temperature of the plastic pool and the following burning behaviours. As the hot-boundary temperature increases, three types of flame were observed subsequently, namely, (I) near-limit flame, (II) transitional flame, and (III) intensive flame. For example, when the boundary temperature was at room temperature (no heating at T_b =25 ℃), the flame of the burning PE melt layer was weak and gentle, mainly showing a blue color (Fig. 4a). This near-limit flame will only be sustained for a short time (less than 30 s) and then quickly quenched by the cold boundary. The plastics also quickly re-solidifies, where the reduction in fuel mass and thickness is very small (see Section 3.4).

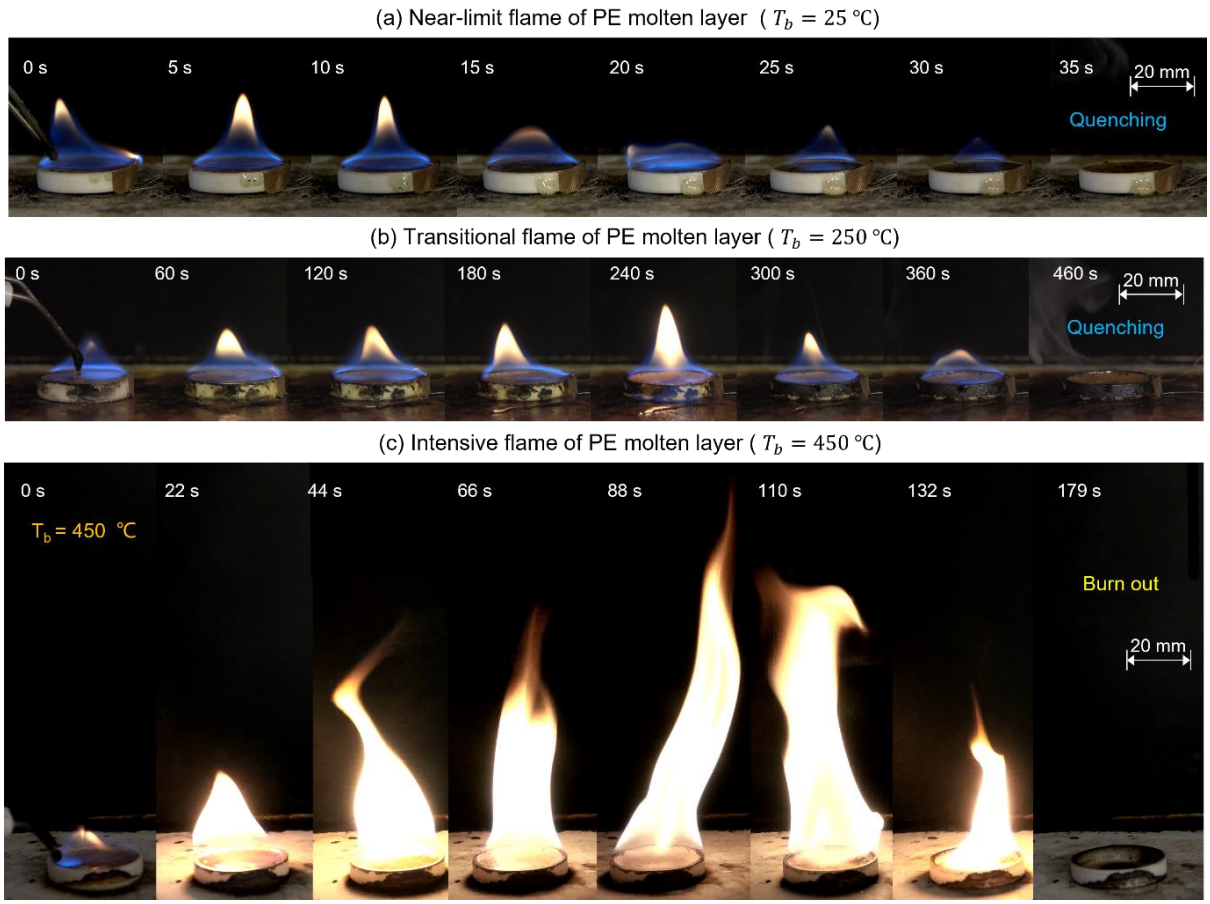

Fig. 4. Molten PE pool fire, (a) near-limit flame without bottom heating, (b) long-lasting transitional flame at 250 ℃ boundary temperature, and (c) the intensive flame of PE molten layer at 450 ℃ boundary temperature, where a spark is used as the pilot source (see Video S2).

Continuing rising the bottom temperature over the melting point of the PE (i.e., T_b >150 ℃), the transitional flame will appear, where the portion of the blue flame is reduced with the increasing boundary temperature (Fig. 4b). Moreover, the sustained time of transitional flame is much longer compared with the near-limit flame, but there is still fuel remaining after extinction that is thinner and molten. The extinction of transitional flame is also caused by quenching. Further increasing the bottom boundary temperature, the molten layer will be bubbling during the burning process, showing an intensive flame (Fig. 4c). The intensive flame has a bright yellow colour and a long, turbulent plume. Finally, the entire molten layer was consumed by flame. Table 2 summarises the detailed characteristics for identifying the three burning patterns.

Table 2. Characteristics of three burning patterns of molten pool fire.

	Flame type	Features	Burning duration	Extinction
I	Near-limit flame (failed ignition)	mostly blue, short and laminar	Short	Quenched
II	Transitional flame	changing from blue to yellow	Increasing with T_b and longest	Quenched
III	Intensive flame	yellow, tall and turbulent plume	Reducing with intensity	Burnout

3.2. Burning duration, flame height, and flashpoint

Fig. 5(a) summarizes the flame burning duration of PE pool fire at different bottom boundary temperatures. Pattern I (near-limit flame) has a shorter flame sustained time. The flame could appear because the dripping melts are hot enough to be ignited. But the flame is difficult to sustain and is quickly quenched by the cold boundary. Thus, Patten I is identified as the failed ignition. Whereas in Pattern II, the flame duration is significantly enhanced. The plastic melts are burning in a mild and stable way, observing as a long-lasting flame. The burning duration in this pattern gradually increases as the bottom temperature increases, so the flame in Pattern II is defined as the transitional flame.

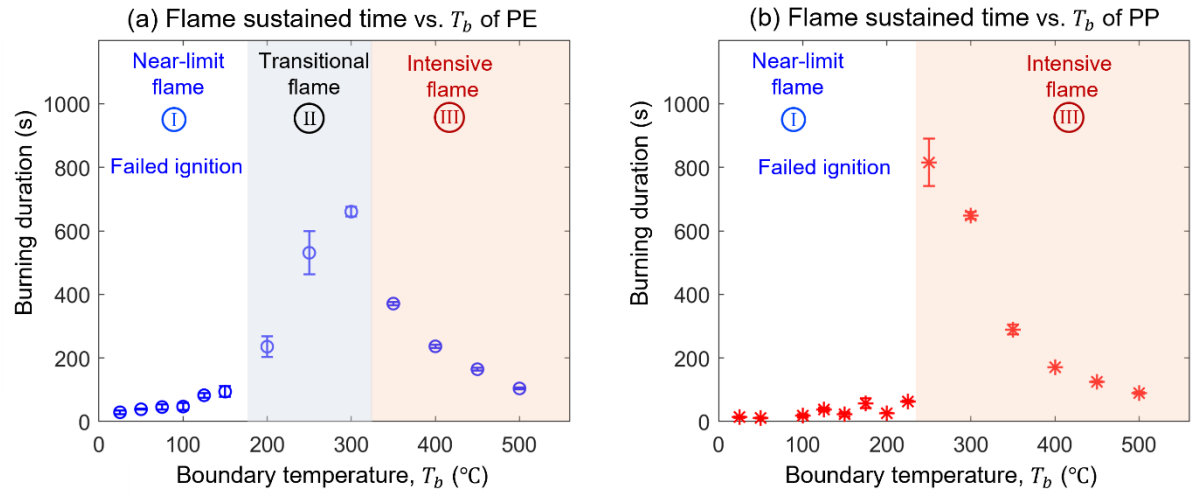

Fig. 5. Flame duration of molten plastic pool fire at different bottom boundary temperatures, (a) 4.8-mm thick PE and (b) 4.5-mm thick PP.

When the boundary temperature continually increases over 310 ℃, the flame duration is gradually reduced with the increasing boundary temperature because of the growing burning intensity. The burning of PP shows similar flaming behaviours, as shown in Fig. 5(b), but the region of Pattern II (long-lasting transitional flame) does not exist or is too small to be observed. Therefore, the sustained time suddenly increases to the longest point without transition.

Different burning patterns also can be easily identified in the flame height evolution diagram. Fig. 6 plots the evolution of flame height under different boundary temperatures for the (a) PE and (b) PP, respectively. For PE, three trends correspond to the three burning patterns in Fig. 6a. For near-limit burning Pattern I (T_b <150 ℃), the flame height is lower than 20 mm, and it quickly diminishes until extinction. For the transitional Pattern II, the flame height reaches the maximum height first and then slowly decreases with time. For the intensive burning Pattern III, the peak flame height is clearly greater than other patterns, appearing as an intensive yellow flame. The burning duration reduces with the boundary temperature because the overall burning rate is enhanced. Then, we can define the flashpoint of plastic pool when an intensive burning Pattern III occurs, that is, 310 ± 10 ℃ for PE. For PP, its burning only shows the near-limit burning Pattern I and the intensive burning Patten III, while the long-lasting transitional (Pattern II) flame is not observed around 200 ℃ (see Fig. 6b).

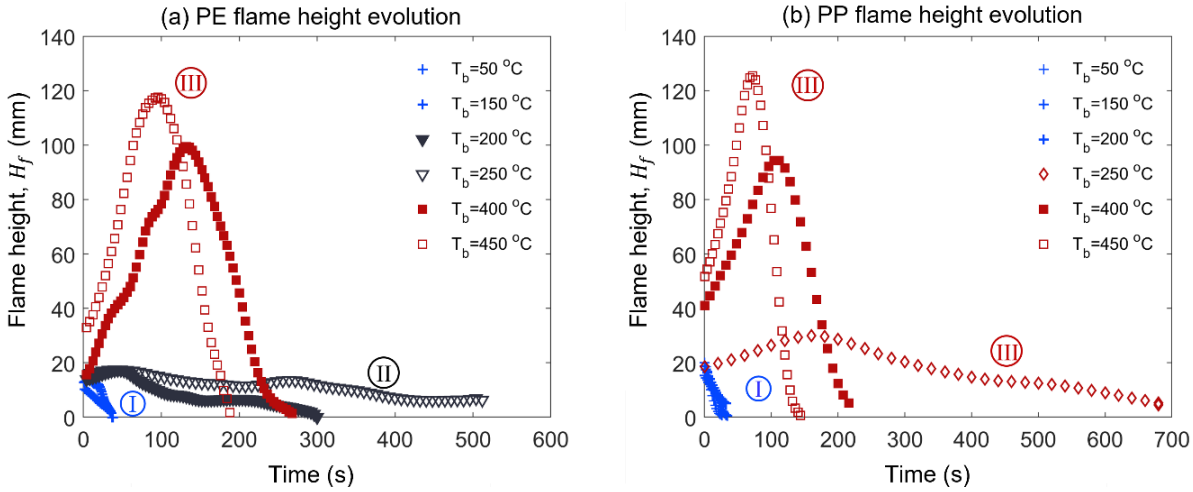

Fig. 6. Flame height of (a) PE and (b) PP at different bottom boundary temperatures.

There are three factors contributing to different burning behaviours between PE and PP pool fires. Frist, the melting point of PP is about 40 ℃ above that of PE. The melting temperature is controlled by the arrangement and nature of the repeating unites for polymer [38]. PE has a lower melting point because of a higher degree of symmetry structure without ramification groups. Consequently, PE is easier to sustain a flame than PP. Secondly, PP has a slightly lower pyrolysis point than PE [39] (see Fig. A1), so it is easier to enter the intensive burning pattern. Thirdly, the liquid components of PP pyrolysis products (i.e., tar) mainly include alkanes and naphthene with molecular chains of C9-C28, while PE pyrolysis liquid products contain larger alkanes, C8-C43 [40]. The hydrocarbons become

harder to ignite as the molecules get bigger, mainly because of the increased latent heat of evaporation and the greater Van der Waals attractions for bigger molecules. Numerical simulations are needed in future work to further quantify influence of these three factors.

When the boundary temperature is over 250 ℃, PP directly enters the intensive burning stage, expressing apparent enhancement of flame height and complete consumption of the molten layer. Thus, the flashpoint of molten PP is 260 ± 10 ℃. The sudden access of Pattern III for PP might be due to its shorter carbon chain and the rapid decomposition rate once ignited [41]. In other words, the PP shows lower thermal stability than PE, which is decided by the presence of methyl group ramification in the PP structure. Moreover, the remaining fuel layer not only includes the liquid virgin plastic, but also contains its liquid products of pyrolysis. Overall, PE is easier to sustain a flame due to a lower melting point, but more difficult to enter the intensive burning pattern due to a harder pyrolysis, showing the transitional flame Pattern. In contrast, PP is either failed to ignite or sustain an intensive flame, and such behaviours are more like a conventional liquid fuel.

3.3. Remaining thickness of molten layer

For Patterns I and II, the flame will be quenched eventually, and partial fuels are remaining. The mass of remaining mass (m_r) is measured by the electric scale after the test. Then, the remaining thickness of the plastic molten layer can be calculated as:

$$\delta = \frac{m_r}{\rho_p \times A} \tag{1}$$

where the density of the polymer (ρ_p) are 920 kg/m^3 for PE [42] and 900 kg/m^3 for PP [43]. Fig. 7 plots the calculated thickness of the molten layer. The red dashed line indicates the original thickness before ignition, which is 4.8 mm for PE and 4.5 mm for PP.

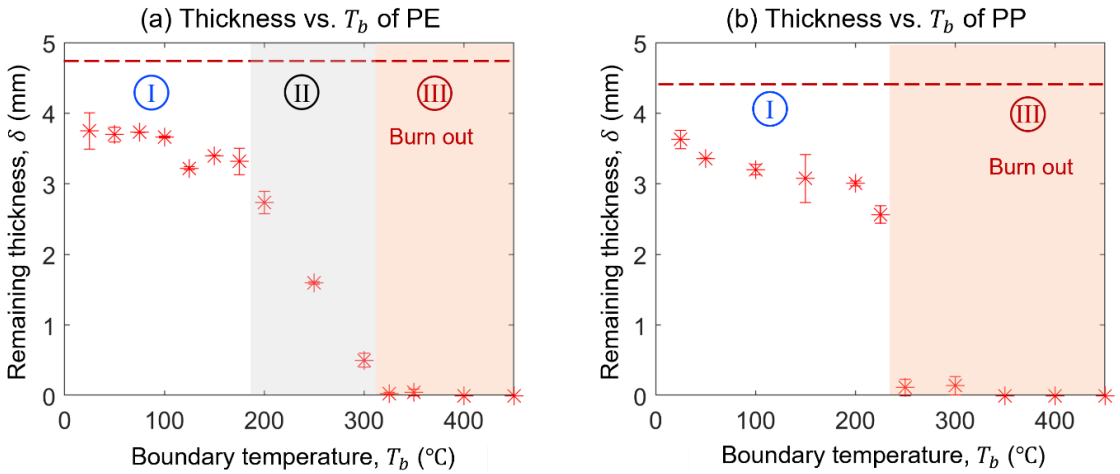

Fig. 7. The remaining thickness of the molten layer for (a) PE and (b) PP, under three burning patterns (I) near-limit flame, (II) long-lasting transition flame, and (III) intensive flame.

For PE in Fig. 7a, when the boundary temperature is in the Pattern I, the remaining thickness is reduced slightly, matching the quickly quenched flame in Pattern I. The remaining thickness gradually reduces with boundary temperature when it is in the range of 175 ℃ to 320 ℃ (Pattern II), which is homologous to the increasing burning rate and longer flame sustained time. For the intensive burning Patter III, all fuels are consumed in the end, so the remaining thickness reduces to zero.

Differently, only two patterns are identified in the burning of PP in Fig. 7b. In Pattern I, the remaining thickness slightly decreases with the increasing boundary temperature. Then, the remaining thickness suddenly drops to zero when the boundary temperature is over 225 ℃, because PP enters the intensive burning stage without the transition. The possible reasons are discussed in Section 3.2.

3.4. Burning flux and heat release rate

As the mass change of the fuel burning is negligible compared to the heavy hot plate, the mass loss cannot be measured directly by a precision scale. Alternatively, the burning rate, represented by the fuel-surface burning mass flux, is estimated by measuring the flame area and flame burning flux [44]. The video processing method is described in the Appendix. Consistent with the trend of flame height, three patterns of burning PE are observed in Fig. 8a. Pattern I (Near-limit flame) has the smallest fuel-surface burning mass flux and the shortest burning duration. For Pattern II (transitional flame), both the burning duration and the burning mass flux increase with the bottom boundary temperature. As expected, Pattern III shows the largest burning flux under both the hottest boundary and intensive flame heating.

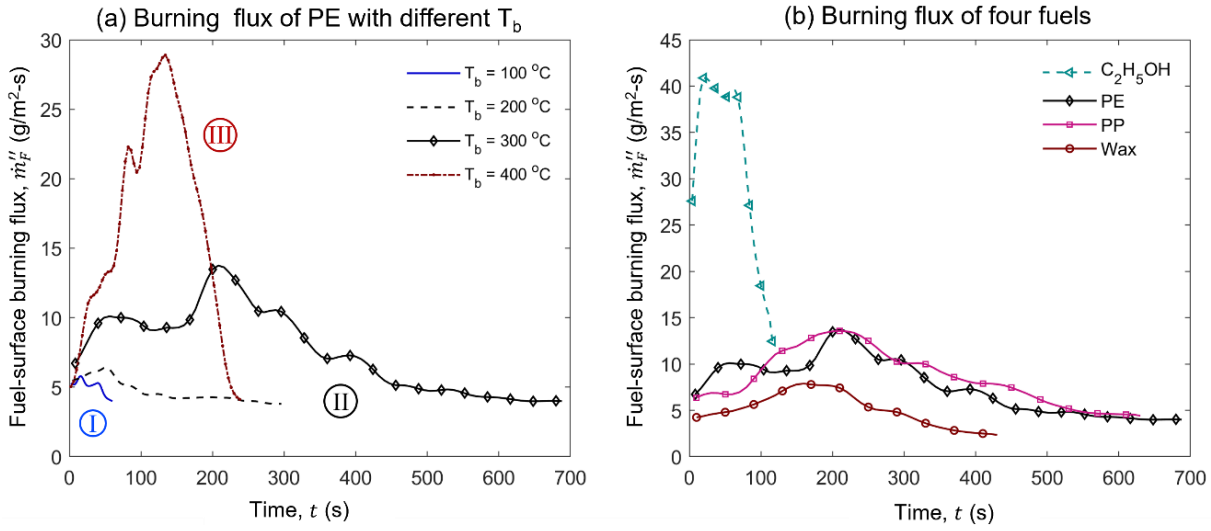

Fig. 8. The burning mass flux, (a) PE under different boundary temperature and (b) comparing four types of fuels, PE, PP, paraffin wax, and ethanol.

Fig. 8b compares the burning rate evolution for four types of fuel under the same boundary temperature (300 ℃). The intensive burning of PE and PP has a similar curve and peak value of the burning rate. The liquid ethanol shows the highest burning rate as expected, because the liquid fuel has a large mass transfer (B) number (see Section 4.2). In fact, the flashpoint, boiling point, and the heat of evaporation for most liquid fuels are much smaller than those for thermoplastics. For the paraffin wax,

its melting point is as low as 50 ℃. However, its flashpoint is around 270 ℃ and comparable to PP, and its boiling point is 350 ± 20 ℃ (see Table 1), lower than the boundary temperature. Therefore, the burning rate of wax is lowest among all fuels.

Fig. 9 summarises the peak burning flux for four different fuels varying with the bottom boundary temperature, where all of them show very different burning patterns and regions. More detailed burning process of four fuels can be found in Supplemental Video S3. For PE in Fig. 9a, the bottom boundary temperature is divided into cooling and heating effect, based on the trend of burning flux in Fig. 8a. Specifically, when the initial bottom temperature is below 300 ℃, the peak burning flux is near-constant and below 10 g/m^2-s, which is decided by the initial temperature of dripping melts. In this temperature span, the boundary cooling is stronger than the flame heating. Thus, the flame is quenched in the end. Over 300 ℃, the cooling from the bottom boundary can be offset by the flame heating from the top, and the latter can further increase the temperature and burning rate of plastic pool.

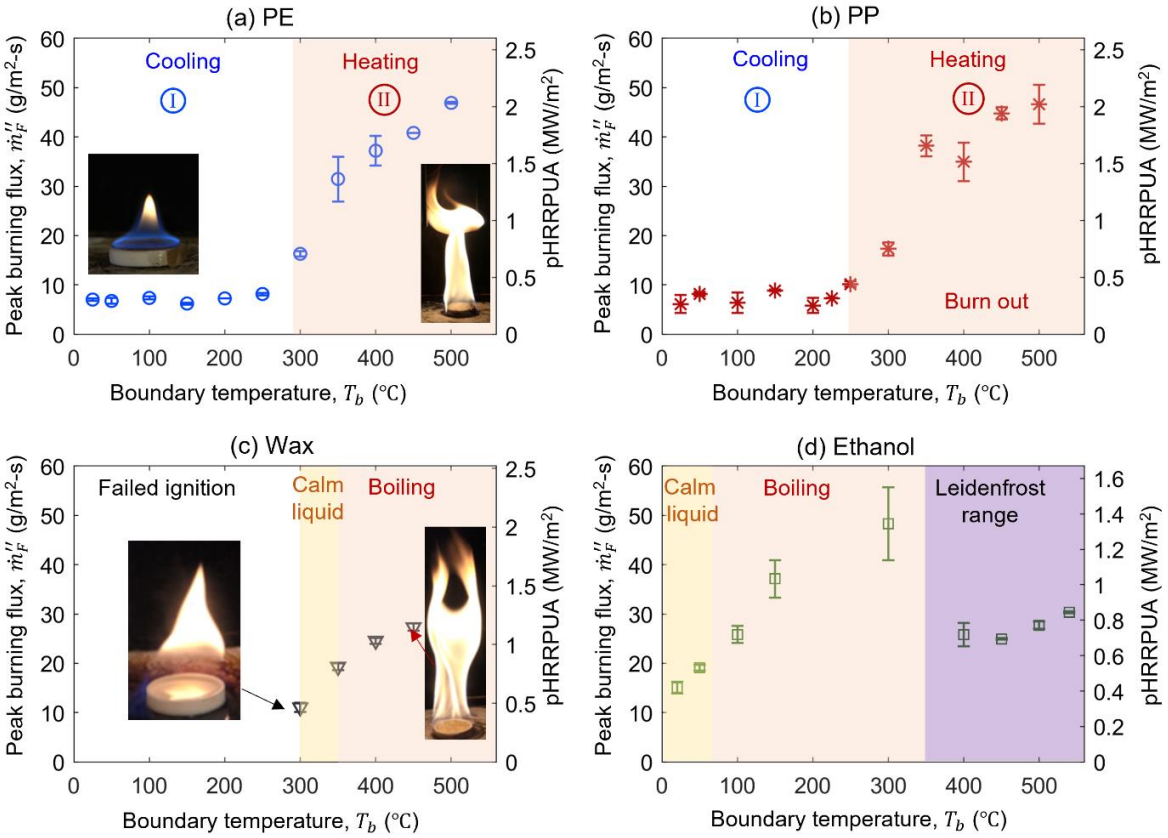

Fig. 9. The burning mass flux and HRR vs. different bottom boundary temperatures, (a) PE, (b) PP, (c) paraffin wax, and (b) ethanol.

Similarly, the burning of PP also shows two regions under different bottom boundary temperatures (Fig. 9b). Below 250 ℃, the peak burning flux is near-constant and below 10 g/m^2-s, indicating that the boundary temperature shows the cooling effect at a low-temperature span. Further increasing the temperature over 250 ℃, the burning intensity is boosted continually, showing a bright yellow flame. In addition, a strong bubbling phenomenon is observed on the top surface inside the intensive flame.

Different from the bubbles found in the conventional boiling process, the observed pyrolysis bubbles on the pool surface are much smaller and can barely move inside the condensed phase.

For wax pool fire (Fig. 9c), the flame can be established successfully when the fuel temperature is over its flashpoint of 270 ± 10 ℃, and no transitional flame is observed. As the wax temperature is slightly lower than the heating boundary, it can sustain a robust flame, when heated by a hot boundary over 300 ℃. Once the pool flame can be sustained, the peak burning flux gradually increases with the increasing boundary temperature. Between 300 ℃ to 350 ℃, the burning wax shows a calm liquid surface during burning. When the fuel is over boiling point, a strong bubbling process can be observed, and the flame becomes intensive and turbulent.

The ethanol can be easily ignited at room temperature because of the lower flashpoint (13 ℃). After the pool fire is established, two types of flame are observed in Fig. 9d, classified by the boiling point of the fuel. For instance, the burning of liquid fuel is much more peaceful when the boundary temperature is below 80 ℃, while over this point, the intensive boiling process is observed at the condensed phase, and the flame becomes turbulent. Moreover, when the temperature is higher than 350 ℃, the Leidenfrost effect is observed for the burning of boiled ethanol. In other words, the film boiling appeared, where a gas layer formed between the liquid fuel and the hot boundary, resisting the conductive heat transfer, so that the burning rate reduces with boundary temperature. However, the Leidenfrost phenomenon was not observed on burning plastic fuels and wax, probably because the boundary temperature in this experiment is not high enough. Such Leidenfrost phenomenon may be observed for plastic pools by further increasing the boundary temperature above 500 ℃.

4. Discussion

4.1. Pool temperature and boundary cooling

In the experiment, the evolution of plastic pool top surface temperature (T_u) was monitored by the IR camera. Fig. 10a shows a group of PE pool surface temperatures during the burning process under different bottom boundary temperatures. In burning Pattern II, the top surface temperature is levelling-off around 450 ℃, when the flame extinction occurs after the long transitional burning. Comparatively, the temperature in Pattern I cannot reach 450 ℃ before it is quickly decayed, because of the stronger cooling from the bottom surface. When the bottom temperature exceeds 450 ℃, the burning enters an intensive burning Pattern III. Bubbles are observed at the top surface. The overall temperature in Pattern III is higher than the other two patterns, and the temperature drop after burnout.

In the long-lasting transitional burning Pattern II, the flame is quenched, when the fuel layer thickness is lower than a specific value. After measuring the temperature evolution for both bottom and top surfaces, we can calculate the heat flux of cooling for the molten layer in pattern II as

$$\dot{q}_c'' = h_{in}\Delta T = Nu\frac{k}{\delta}(T_u - T_b) \quad (2)$$

where T_u and T_b are temperatures of plastic pool top and bottom surfaces, respectively; δ indicates the thickness of the molten layer, which is regressing gradually with the burning process. Based on the burning flux in Fig. 8a, the transient conductive heat loss can be calculated and plotted.

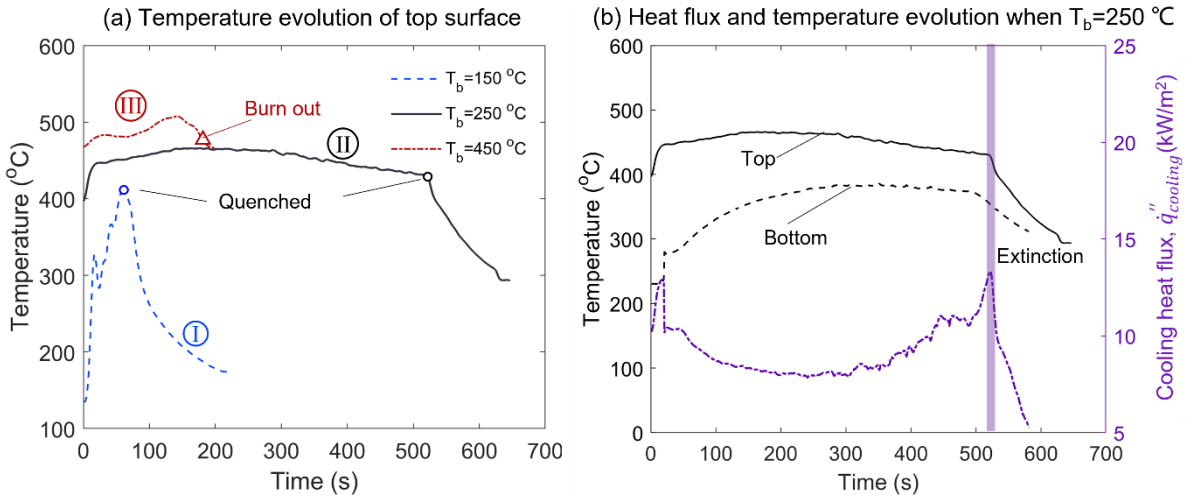

Fig. 10. Temperature evolution of PE molten layer for (a) top surface under three burning patterns and (b) top and bottom surface under a transitional flame and the calculated cooling heat flux.

Fig. 10b shows the measured T_u and T_b and the calculated $\dot{q}_c''$ of PE pool when the boundary temperature is 250 ℃. Initially, the top surface temperature is much greater than the bottom temperature, because of the flame heating, showing a relatively large cooling flux. When the flame becomes weaker, the temperature difference (ΔT) approaches a constant before flame extinction, indicating a steady burning state. Because the thickness of the molten layer decreases continually, the heat flux of cooling increases. Finally, the flame has been quenched. When the transitional flame is extinguished, the cooling heat flux is 14 kW/m^2 with a 1.5 mm final fuel thickness (see Fig. 7). This result gives useful information in preventing the self-sustained plastic pool fire. When the boundary temperature is in the transitional region, it is important to reduce the fuel thickness lower than the critical thickness for quenching. In this way, the fire risk of long-lasting plastic pool fires can be significantly reduced.

4.2. Heat transfer analysis

A simplified one-dimensional heat and mass transfer model is applied to analyse the boundary effects on the burning of the molten layer. According to the burning rate of the stagnant layer model [45], the burning rate of the hot molten layer can be estimated using the mass transfer number as

$$\dot{m}_F'' = \frac{h}{c_p}\ln(1+B) \qquad (3a)$$

where B is the mass-transfer number, c_p is the specific heat of molten plastics, and h is the convective heat transfer coefficient. As the molten plastic layer is in the liquid phase and always hotter than the boundary layer, the Nusselt number is adopted to correlate the heat transfer coefficient [45] as

$$Nu = 0.54\, Ra^{\frac{1}{4}} \quad (10^4 < Ra < 10^7, Pr > 0.7) \tag{4}$$

Then, the burning rate equation becomes

$$\dot{m}_F'' = 0.54 Ra^{\frac{1}{4}} \frac{k}{\delta c_p} ln(1+B) \tag{3b}$$

The cooling effect from the bottom boundary shows a great impact on the mass transfer number. Then, B number should be modified by adding the additional heat loss.

$$B = \frac{\Delta h_c / \nu - c_{pg}(T_{py} - T_\infty)}{\Delta h_{py} - Q} \tag{5}$$

where Δh_c is the heat of combustion; ν *is* the stoichiometric air-fuel ratio; T_{py} and T_∞ is the pyrolysis temperature and the ambient temperature separately; the resistance of mass transfer process includes the Δh_{py} is pyrolysis heat and the thermal inertia. Q is the thermal inertia driven by the heat transfer process on the top surface of plastic pool.

$$Q = \frac{\dot{q}_f'' - \dot{q}_{re,r}'' - \dot{q}_c''}{\dot{m}_F''} \tag{6}$$

where $\dot{q}_f''$ is the heat flux from the flame, $\dot{q}_{re,r}''$ is the re-radiative heat loss, and $\dot{q}_c''$ is the cooling from the bottom boundary layer in Eq. (2).

For Pattern I near-limit flame, the flame is weak and mostly blue, showing limited heating ability. On the other hand, the temperature difference between the top and the bottom boundary is larger, which means the cooling from the bottom boundary might dominate the burning intensity. With the increasing boundary temperature, the cooling from the bottom boundary is reduced. Then, the value of $\dot{q}_c''$ is reduced in Eq. (6), resulting in the larger value of thermal inertia Q. Back to Eq. (5), the increasing thermal inertia induces a larger B number. Similarly, the B number continually increased with the boundary temperature for the burning Pattern II. For the intensive burning Pattern III, the flame heating flux ($\dot{q}_f''$) controls the burning rate, and it dramatically increases with the boundary temperature and flame size. Thus, as the boundary temperature increases, the B number increases, and the burning rate keeps increasing in Pattern III.

5. Conclusions

This work investigates the burning behaviours and quantifies the fire hazards of the accumulated molten drips. The burning of PE pool shows three burning patterns: when the boundary temperature is lower than the melting point of PE, burning Pattern I (near-limit blue flame or failed ignition) appears shortly before quenching. Above the melting point, the flame becomes more robust and lasts for a longer period (Pattern II: transitional flame). After quenching, a thin layer fuel remains, and its thickness decreases with the increasing boundary temperature. When the plastic pool exceeds its flashpoint, the

burning becomes intensive with a yellow flame to burn out the fuel (Pattern III: intensive flame). PP does not have this transitional-flame stage due to a higher melting point and lower pyrolysis point.

The boundary temperature can be divided into cooling and heating regions for the plastic pool fire. At the cooling region, the cooling effect is dominated the burning process. Thus, the flame is finally quenched by the cold boundary. Over its flashpoint, the peak burning flux start to increase with the boundary temperature. The boundary temperature would promote the burning intensity, showing a greater fire risk. Different from the boiling process in the pool fire of wax and ethanol, the plastic pool fire only shows the bubbling process on the top surface, and the pyrolysate bubbles are much smaller that can barely move inside the condensed phase. This study promotes the understanding of the melting and burning of plastics in real fire scenarios and helps quantify hazards of dripping and flooring fires.

Acknowledgments

This research is supported by the Hong Kong Research Grant Council through the Early Career Scheme (25205519), Shanghai Science and Technology Committee (19160760700), and the General Program of Shenzhen Science and Technology Innovation Commission (JCYJ20210324131006017).

CRediT authorship contribution statement

Peiyi Sun: Methodology, Data curation, Investigation, Resources, Writing - Original Draft.

Xinyan Huang: Conceptualization, Methodology, Funding acquisition, Supervision, Writing - Review & Editing.

Cansu Xu: Methodology, Resources, Investigation, Supervision.

References

[1] A. Tewarson, Flammability of Polymers, in: Plastics and the Environment, John Wiley & Sons, Ltd, Hoboken, NJ, USA, 2004: pp. 403–489. https://doi.org/10.1002/0471721557.ch11.

[2] G. Kernick, Catastrophe and systemic change: Learning from the Grenfell Tower fire and other disasters, Do Sustainability, 2021.

[3] T. Ohlemiller, J. Shields, Aspects of the fire behavior of thermoplastic materials, 2008.

[4] S. Luo, Q. Xie, X. Tang, R. Qiu, Y. Yang, A quantitative model and the experimental evaluation of the liquid fuel layer for the downward flame spread of XPS foam, Journal of Hazardous Materials. 329 (2017) 30–37. https://doi.org/10.1016/j.jhazmat.2017.01.028.

[5] A. Tewarson, R.F. Pion, Flammability of plastics-I. Burning intensity, Combustion and Flame. 26 (1976) 85–103. https://doi.org/10.1016/0010-2180(76)90059-6.

[6] E.M. Sparrow, G.T. Geiger, Melting in a horizontal tube with the solid either constrained or free to fall under gravity, International Journal of Heat and Mass Transfer. 29 (1986) 1007–1019. https://doi.org/10.1016/0017-9310(86)90200-0.

[7] S. Singh, Y. Nakamura, A Numerical Study of Dripping on the Ignitability of a Vertically Oriented Thermoplastic Material Locally Heated by an Irradiation Source, Fire Technology.

(2021). https://doi.org/10.1007/s10694-021-01137-7.

[8] J. Zhang, T.J. Shields, G.W.H. Silcock, Effect of Melting Behaviour on Upward Flame Spread of Thermoplastics, Fire and Materials. 21 (1997) 1–6. https://doi.org/10.1002/(sici)1099-1018(199701)21:1<1::aid-fam583>3.3.co;2-g.

[9] P. Sun, S. Lin, X. Huang, Ignition of thin fuel by thermoplastic drips: An experimental study for the dripping ignition theory, Fire Safety Journal. 115 (2020) 103006. https://doi.org/10.1016/j.firesaf.2020.103006.

[10] P. Sun, Y. Jia, X. Zhang, H. Xinyan, Fire Risk of Dripping Flame: Piloted Ignition and Soaking Effect, Fire Safety Journal. (2021) 103360. https://doi.org//10.1016/j.firesaf.2021.103360.

[11] P. Sun, A. Rodriguez, W. Il Kim, X. Huang, C. Fernandez-Pello, Effect of external and internal heating on the flame spread and phase change of thin polyethylene tubes, International Journal of Thermal Sciences. 168 (2021) 107054. https://doi.org/10.1016/j.ijthermalsci.2021.107054.

[12] UL 94, Tests for Flammability of Plastic Materials for Parts in Devices and Appliances, Ul. (2013). https://standardscatalog.ul.com/standards/en/standard_94_6.

[13] EN-13823:2010+A1:2014, BSI Standards Publication: Reaction to fire tests for building products — Building products excluding floorings exposed to the thermal attack by a single burning item, 2014.

[14] Y. Wang, J. Jow, K. Su, J. Zhang, Dripping behavior of burning polymers under UL94 vertical test conditions, Journal of Fire Sciences. 30 (2012) 477–501. https://doi.org/10.1177/0734904112446125.

[15] Y. Wang, J. Zhang, Thermal stabilities of drops of burning thermoplastics under the UL 94 vertical test conditions, Journal of Hazardous Materials. 246–247 (2013) 103–109. https://doi.org/10.1016/j.jhazmat.2012.12.020.

[16] B.K. Kandola, D. Price, G.J. Milnes, A. Da Silva, Development of a novel experimental technique for quantitative study of melt dripping of themoplastic polymers, Polymer Degradation and Stability. 98 (2013) 52–63. https://doi.org/10.1016/j.polymdegradstab.2012.10.028.

[17] B.K. Kandola, M. Ndiaye, D. Price, Quantification of polymer degradation during melt dripping of thermoplastic polymers, Polymer Degradation and Stability. 106 (2014) 16–25. https://doi.org/10.1016/j.polymdegradstab.2013.12.020.

[18] Y. Kim, A. Hossain, Y. Nakamura, Numerical modeling of melting and dripping process of polymeric material subjected to moving heat flux: Prediction of drop time, Proceedings of the Combustion Institute. 35 (2015) 2555–2562. https://doi.org/10.1016/j.proci.2014.05.068.

[19] C. Xiong, X. Huang, Numerical Modeling of Flame Shedding and Extinction behind a Falling Thermoplastic Drip, Flow, Turbulence and Combustion. 107 (2021) 745–758. https://doi.org/10.1007/s10494-021-00250-5.

[20] X. Huang, Critical Drip Size and Blue Flame Shedding of Dripping Ignition in Fire, Scientific

Reports. 8 (2018) 16528. https://doi.org/10.1038/s41598-018-34620-3.

[21] Bangkok Post, Fire causes blackout on Sukhumvit 31, (2020). https://www.bangkokpost.com/thailand/general/2019591/fire-causes-blackout-on-sukhumvit-31.

[22] ITV, Fire services at Cineworld on Broad Street after light catches fire | Central - ITV News, (2015). https://www.itv.com/news/central/update/2015-12-06/fire-services-at-cineworld-on-broad-street-after-light-catches-fire/ (accessed March 25, 2022).

[23] G. Xiong, D. Zeng, A. Krisman, Y. Wang, On the burning behavior of thermoplastics at large scale: Uncartoned unexpanded plastic commodity, Fire Safety Journal. 120 (2021) 103089. https://doi.org/10.1016/j.firesaf.2020.103089.

[24] V. Babrauskas, U.G. Wickström, Thermoplastic pool compartment fires, Combustion and Flame. 34 (1979) 195–202. https://doi.org/10.1016/0010-2180(79)90092-0.

[25] Q. Xie, R. Tu, N. Wang, X. Ma, X. Jiang, Experimental study on flowing burning behaviors of a pool fire with dripping of melted thermoplastics, Journal of Hazardous Materials. 267 (2014) 48–54. https://doi.org/10.1016/j.jhazmat.2013.12.033.

[26] Q. Xie, H. Zhang, R. Ye, Experimental study on melting and flowing behavior of thermoplastics combustion based on a new setup with a T-shape trough, Journal of Hazardous Materials. 166 (2009) 1321–1325. https://doi.org/10.1016/j.jhazmat.2008.12.057.

[27] X. Wang, X. Cheng, L. Li, S. Lo, H. Zhang, Effect of ignition condition on typical polymer's melt flow flammability, Journal of Hazardous Materials. 190 (2011) 766–771. https://doi.org/10.1016/j.jhazmat.2011.03.108.

[28] A.T. Modak, P.A. Croce, Plastic pool fires, Combustion and Flame. 30 (1977) 251–265. https://doi.org/10.1016/0010-2180(77)90074-8.

[29] A. Vali, D.S. Nobes, L.W. Kostiuk, Transport phenomena within the liquid phase of a laboratory-scale circular methanol pool fire, Combustion and Flame. 161 (2014) 1076–1084. https://doi.org/10.1016/j.combustflame.2013.09.028.

[30] A. Byström, X. Cheng, U. Wickström, M. Veljkovic, Measurement and calculation of adiabatic surface temperature in a full-scale compartment fire experiment, Journal of Fire Sciences. 31 (2013) 35–50. https://doi.org/10.1177/0734904112453012.

[31] U. Hujuri, A.K. Ghoshal, S. Gumma, Modeling pyrolysis kinetics of plastic mixtures, Polymer Degradation and Stability. 93 (2008) 1832–1837. https://doi.org/10.1016/j.polymdegradstab.2008.07.006.

[32] N. Wang, R. Tu, X. Ma, Q. Xie, X. Jiang, Melting behavior of typical thermoplastic materials - An experimental and chemical kinetics study, Journal of Hazardous Materials. 262 (2013) 9–15. https://doi.org/10.1016/j.jhazmat.2013.08.024.

[33] Y. Yao, E. Chau, G. Azimi, Supercritical fluid extraction for purification of waxes derived from polyethylene and polypropylene plastics, Waste Management. 97 (2019) 131–139. https://doi.org/10.1016/j.wasman.2019.08.003.

[34] S. Dillon, A. Hamins, Ignition Propensity and Heat Flux Profiles of Candle Flames for Fire

Investigation, Fire Science Applications to Fire Investigations. (2003) 363–376. http://fire.nist.gov/bfrlpubs/fire03/PDF/f03032.pdf.

[35] R. Dai, G. Chandrasekaran, J. Chen, C. Jackson, Y. Liu, Q. Nian, B. Kwon, Thermal conductivity of metal coated polymer foam: Integrated experimental and modeling study, International Journal of Thermal Sciences. 169 (2021) 107045. https://doi.org/10.1016/J.IJTHERMALSCI.2021.107045.

[36] Jalaluddin, A. Miyara, Thermal performance investigation of several types of vertical ground heat exchangers with different operation mode, Applied Thermal Engineering. 33–34 (2012) 167–174. https://doi.org/10.1016/J.APPLTHERMALENG.2011.09.030.

[37] B. Shen, T. Hamazaki, W. Ma, N. Iwata, S. Hidaka, A. Takahara, K. Takahashi, Y. Takata, Enhanced pool boiling of ethanol on wettability-patterned surfaces, Applied Thermal Engineering. 149 (2019) 325–331. https://doi.org/10.1016/J.APPLTHERMALENG.2018.12.049.

[38] M. Paraschiv, R. Kuncser, M. Tazerout, T. Prisecaru, New energy value chain through pyrolysis of hospital plastic waste, Applied Thermal Engineering. 87 (2015) 424–433. https://doi.org/10.1016/j.applthermaleng.2015.04.070.

[39] A. Aboulkas, K. El harfi, A. El Bouadili, Thermal degradation behaviors of polyethylene and polypropylene. Part I: Pyrolysis kinetics and mechanisms, Energy Conversion and Management. 51 (2010) 1363–1369. https://doi.org/10.1016/j.enconman.2009.12.017.

[40] G. Yan, X. Jing, H. Wen, S. Xiang, Thermal cracking of virgin and waste plastics of PP and LDPE in a semibatch reactor under atmospheric pressure, Energy and Fuels. 29 (2015) 2289–2298. https://doi.org/10.1021/ef502919f.

[41] Y. Quan, Z. Zhang, R. Tanchak, Q. Wang, A review on cone calorimeter for assessment of flame retarded polymer composites, Journal of Thermal Analysis and Calorimetry. (2022). https://doi.org/10.1007/s10973-022-11279-7.

[42] S. Ronca, Chapter 10 - Polyethylene, in: Brydson's Plastics Materials, 8th ed., Elsevier Ltd, 2017: pp. 247–278. https://doi.org/10.1016/B978-0-323-35824-8.00010-4.

[43] S. Mazloum, Y. Aboumsallem, S. Awad, N. Allam, K. Loubar, Modelling pyrolysis process for PP and HDPE inside thermogravimetric analyzer coupled with differential scanning calorimeter, International Journal of Heat and Mass Transfer. 176 (2021) 121468. https://doi.org/10.1016/j.ijheatmasstransfer.2021.121468.

[44] P. Sun, C. Wu, F. Zhu, S. Wang, X. Huang, Microgravity combustion of polyethylene droplet in drop tower, Combustion and Flame. 222 (2020) 18–26. https://doi.org/10.1016/j.combustflame.2020.08.032.

[45] J.G. Quintiere, Fundamentals of fire phenomena, John Wiley, 2006.

Appendix

The plastic sample was grinded into powders for thermogravimetric analysis (TGA) analysis, using PerkinElmer STA 6000 Simultaneous Thermal Analyzer. The initial mass of PE and PP sample is 2-3 mg. The sample were heated at the constant rates of 30 ℃/min and 60 ℃/min. Two oxygen concentrations were selected, 0% (nitrogen) and 21% (air), with a flow rate of 20 mL/min. The repeating tested were conducted to ensure the repeatability of the testing results. Fig. A1 shows the mass-loss rate (DTG) and the heat flow curve (DSC) for PE and PP, respectively. Regardless the oxygen concentration, the rapidly increasing mass loss rate is around 370±10 ℃ for PE and 340±10 ℃ for PP, which indicates the pyrolysis point of these two thermoplastics. In DSC curves, the melting point can be identified where the PE has the lower meting temperature than PP.

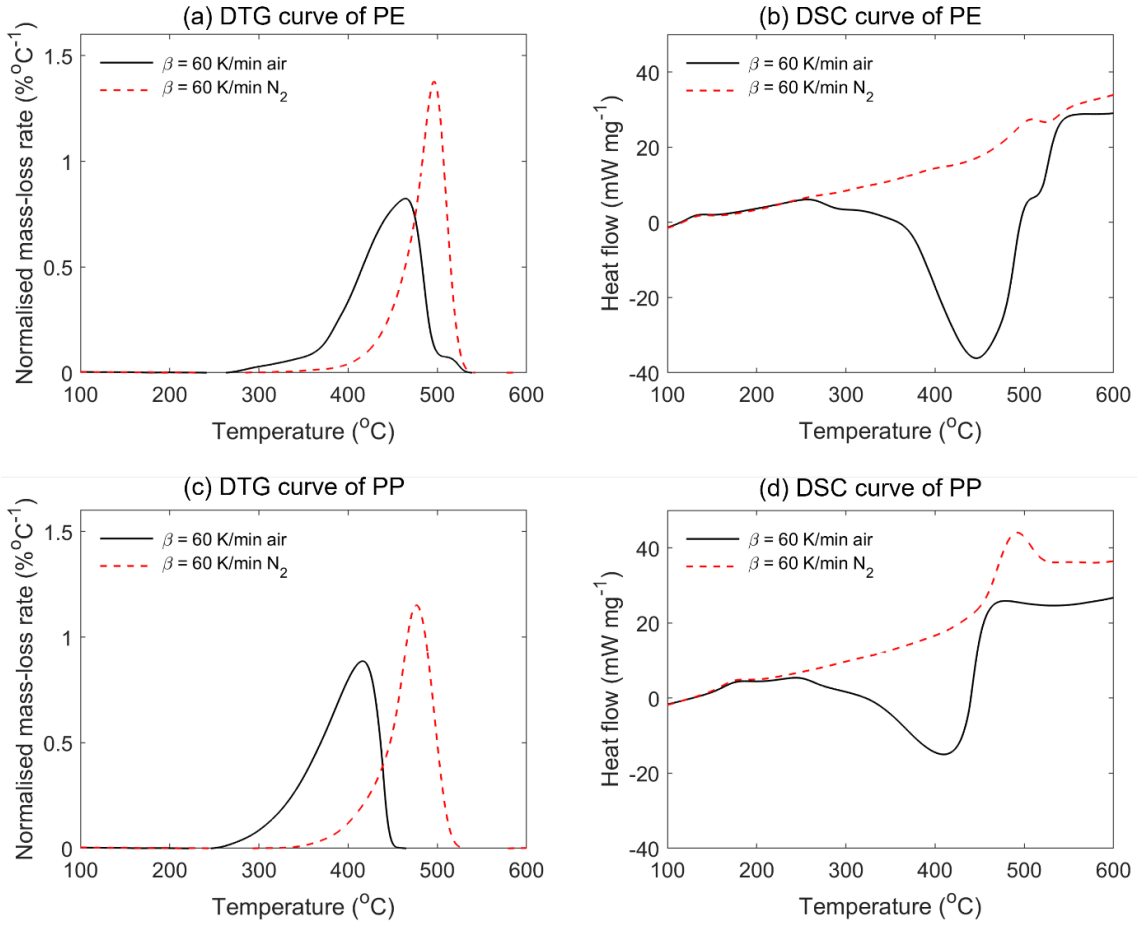

Fig. A1. TGA-DSC results of thermoplastic sample under air and nitrogen flow at the heating rate of 30 K/min and 60 K/min, normalized mass loss rate for (a) PE and (c) PP; heat flow as a function of temperature for (b) PE and (d) PP.

The burning mass rate can be estimated by quantifying the flame area and flame mass flux. The flame sheet is simplified into an axis symmetrical shape. Although the camera only captures the 2-D pictures, and the flame is in a 3-D geometry, the flame surface can be estimated using the symmetry property of the flame shell. In other words, the total flame area consists of several cylindrical side

surfaces along the flame height as

$$A_f = \sum \pi(x_1 - x_2)\delta\gamma^2 \quad (A1)$$

Where the x_1 and x_2 is the sequence number of the pixel at horizontal direction; δ is the thickness of each flame shell ring, we choose one-pixel thickness for this study; γ is the length to pixel ratio, which is 0.06 mm/pixel. A Python code was developed to help process the video to get the flame area of each burning scenario.

The flame mass flux ($\dot{m}_f''$) is defined as the ratio of fuel-burning rate to the flame sheet area. Without the heavy hot plate, the mass loss of plastic melts can be directly measured by an electric scale with 0.001g accuracy. Moreover, the plastic melts are burning on the rock wool board. In this way, a stable plastic pool flame is observed, because the rock wool has the larger permeability and low conductivity, which are benefits to sustain the plastic pool fire at room temperature [10]. By measuring the average flame area and mass loss within this period, the mass loss related to the unit flame area can be calculated. Table A1 shows the flame area and the mass loss rate in quantifying the base flame mass flux for four fuels. The flame burning flux for PE, PP, wax and ethanol were measured as 3.8 g/m^2-s, 4.2 g/m^2-s, 2.0 g/m^2-s and 5.6 g/m^2-s separately.

Table A1. Measurements of base flame mass flux for four fuels, where the relative uncertainty is 10%.

	PE	PP	wax	Ethanol
Flame sheet area (mm^2)	1042	875	394	1651
Total mass loss (g)	0.30	0.28	0.06	1.45
Burning duration (s)	75	75	75	156
Flame burning flux (g/m^2-s)	3.8	4.2	2.0	5.6

Finally, the fuel-surface burning mass flux ($\dot{m}_F''$) under different boundary temperatures can be estimated as

$$\dot{m}_F'' = \frac{A_f}{A_F}\dot{m}_f'' \quad (A2)$$

where A_f is the flame shell area; $\dot{m}_f''$ is the fuel mass flux on the flame sheet; A_F is the fuel surface area, which equals the cross-sectional area of the crucible. Fig. A2 shows the flame area and the estimated burning rate under three boundary temperatures. When the mass flux lower than 4.5 g/m^2-s, the flame was oscillated and became unstable, indicating the burning entered the near quenching stage. The extinction happened when the burning mass flux is lower than 4 g/m^2-s.

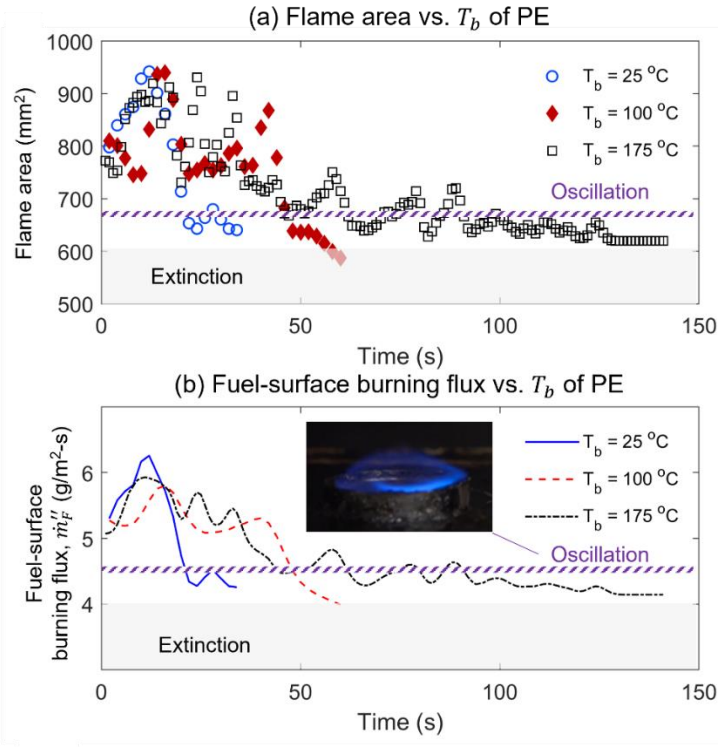

Fig. A2. PE molten layer under three boundary temperatures, (a) measure the equivalent flame area, and (b) fuel-surface burning flux ($\dot{m}''_F$).